

## PLASTIC DEFORMATION AND DISLOCATIONS IN Al-BASED CUBIC INTERMETALLICS

Kei-ichi FUKUNAGA\*, Masayuki HASHIMOTO\*, Kazuhiro YAMADA\*\* and Yasuhiro MIURA\*\*

\*Graduate student, Kyushu University

\*\*Department of Materials Science and Engineering, Kyushu University  
Hakozaki, Higashi-ku, Fukuoka, 812-8581 Japan

**ABSTRACT** Yield strength of the  $L1_2$ -(Al,Ni)<sub>3</sub>Ti alloys showed a marked increase in the low temperature range and a slight increase in the high temperature range. A jerky flow is observed in compressive deformation at intermediate temperature (~500K) and with strain rate  $\sim 10^{-4}$ /s. The critical strain for the onset of jerky flow depends on strain rate and test temperature. Plastic deformation of these alloys occurs by the motion of superdislocations with  $a\langle 110 \rangle$  gliding on  $\{111\}$  planes. Dissociation of superdislocations in (Al,Ni)<sub>3</sub>Ti is of APB (anti-phase boundary) type on  $\{001\}$  plane at high temperature (1073K).

**Keywords:**  $L1_2$  intermetallics, jerky flow, superdislocations, partial dislocations, anti-phase boundary.

### 1. INTRODUCTION

$L1_2$ -(Al,X)<sub>3</sub>Ti intermetallics are known to have low density and good oxidation resistance to high temperature, but these alloys show little tensile ductility at room temperature. The previous experimental results on the deformation characteristic and the nature of dislocation in these alloys are not always consistent. Further experimental study is necessary for the complete understanding of the characteristic properties of the alloys. In the present study, compressive yield strength was measured and observation of dislocation structure was made in ternary (Al,Ni)<sub>3</sub>Ti deformed at various temperatures.

### 2. EXPERIMENTAL PROCEDURE

Polycrystalline  $L1_2$ -(Al,Ni)<sub>3</sub>Ti alloys were prepared by nonconsumable electrode arc melting. The nominal composition of these alloys are  $Al_{67}Ni_8Ti_{25}$ . The arc melted alloy buttons were sealed in silica tubes with high purity Ar gas and subjected to homogenizing treatment at 1373K for  $3.6 \times 10^5$ s. The specimen after heat treatment are confirmed to be  $L1_2$  single phase using by X-ray analysis. Specimens for compressive test were prepared from the heat-treated buttons by using an electro-discharge cutting machine (3mm diameter and 6mm length). Compression tests were carried out between 77K and 1100K, with initial strain rate  $\sim 10^{-4}$ s<sup>-1</sup>. Thin plates were cut perpendicular to the deformation axis and foils for electron microscopic observation were prepared by twin-jet electropolishing with a 25vol% HNO<sub>3</sub>-methanol solution at 223K. Dark field reflections were used for usual observation. An electron microscope JEM-200CX of the HVEM Laboratory of Kyushu

University was used.

### 3. RESULTS AND DISCUSSION

#### 3.1 Strength

Figure 1 shows stress-strain curves from compression test for  $Al_{67}Ni_8Ti_{25}$  deformed at 77-1083K. Nearly 2% of compressive strain was measured before the initiation of crack at low temperature range. The strain of failure is smaller than that of other  $Li_2-(Al,X)_3Ti$  alloys. Cracks of specimens after fracture were parallel to compressive axis. Yield stress of  $Al_{67}Ni_8Ti_{25}$  was higher than that of Cr modified  $Al_3Ti$ [1] at all test temperatures. The temperature dependence of the yield stress ( $\sigma_{0.2}$ ) decreases with increasing temperature from 77K to room temperature. From RT to 672K,  $\sigma_{0.2}$  shows a slight positive temperature dependence. Above 672K,  $\sigma_{0.2}$  decreases gradually.

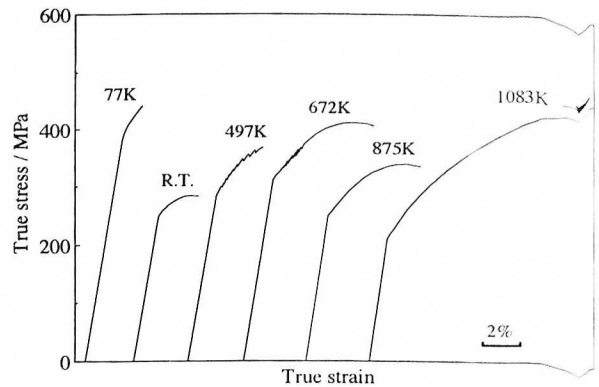


Fig.1 Compression stress-strain curves for  $(Al,Ni)_3Ti$  alloy.

#### 3.2 Jerky flow

The most noticeable feature of the stress-strain curves is the occurrence of serration at intermediate temperature, as illustrated in Fig. 1. At temperatures higher than 873K, no jerky flows were observed in the stress-strain curves. The critical strain ( $\epsilon_c$ ) for the onset of jerky flow depends on strain rate ( $\dot{\epsilon}$ ) and test temperature (T). Higher temperature and smaller strain rate result in smaller critical strain, as is shown in Fig. 2. This strongly suggests that the observed serrated flow is caused by dynamic strain aging due to the interaction of solute atoms with moving dislocations.

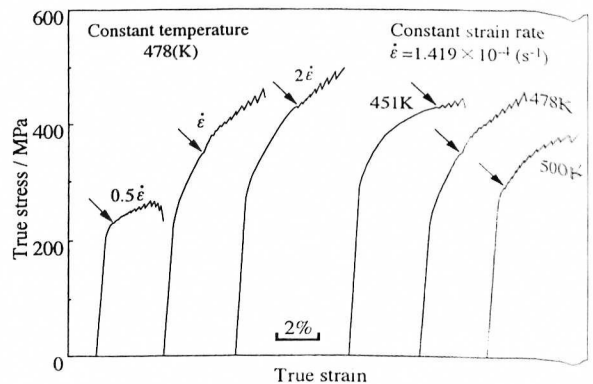


Fig.2 Compression stress-strain curves for  $(Al,Ni)_3Ti$ . The arrows indicate the onset of serrated flow.

In the followings, analysis is made of the experimental results according to the classical theory of dynamic strain aging by Cottrell[2] and Ham and Jaffrey[3]. Serrated flow starts when the velocity of mobile dislocations becomes approximately equal to the diffusion velocity of solute atoms. The following equation holds.

$$\dot{\epsilon} = A \frac{\epsilon_c^{m+r}}{T} \exp\left(-\frac{Q}{kT}\right) \quad (1)$$

where  $A$  is constant,  $k$  is Boltzmann constant and  $T$  is absolute temperature. The vacancy concentration and dislocation density is expressed by the equations,  $C_v = B\epsilon^m$  and  $r = Ne^f$ , respectively.  $B$  and  $N$  are the constants. The activation energy  $Q_m$  is estimated to be about 130kJ/mol, which is much smaller than the lattice diffusion of substitutional atoms. Diffusion in ordered lattices is generally expected to be much slower than in the disordered, because diffusing atoms tend to leave behind traces of disordered region where thermodynamical equilibrium is not maintained.[4] That low activation energy lead to an idea that the controlling process is the diffusion of certain interstitial solute atoms.

### 3.3 Dislocation structure

The dislocation structures of undeformed specimen revealed by TEM are shown in Fig.3. Networks and subgrain boundaries which are one of the thermal stable structures are shown, and dislocation density are very low. Burgers vector of dislocations in Fig.3 are determined to be  $b // \langle 110 \rangle$  and  $b // \langle 100 \rangle$ , but dissociation of that dislocation are not shown.

Fig.4 shows dark field micrograph showing dislocations in the  $Al_{67}Ni_8Ti_{25}$  alloys deformed to 0.5% at 773K. Dislocations in specimens distributes homogeneously. Burgers vectors of the dislocations indicated by A and B in Fig.4 are determined to be respectively  $b = a\langle 110 \rangle$  and  $b = a\langle 100 \rangle$ , where  $a$  is lattice constant.

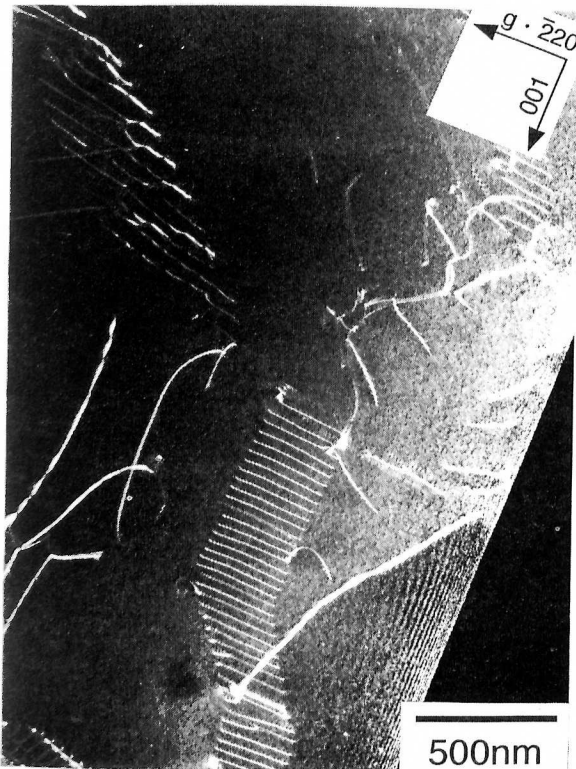


Fig.3 Dark field electron micrograph showing dislocations in undeformed  $(Al,Ni)_3Ti$ .

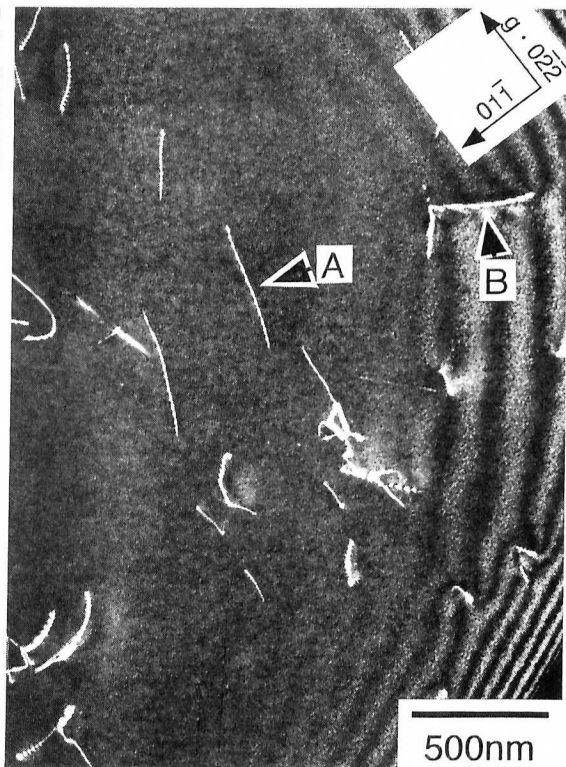


Fig.4 Dark field electron micrograph showing dislocations in  $(Al,Ni)_3Ti$  deformed at 773K.

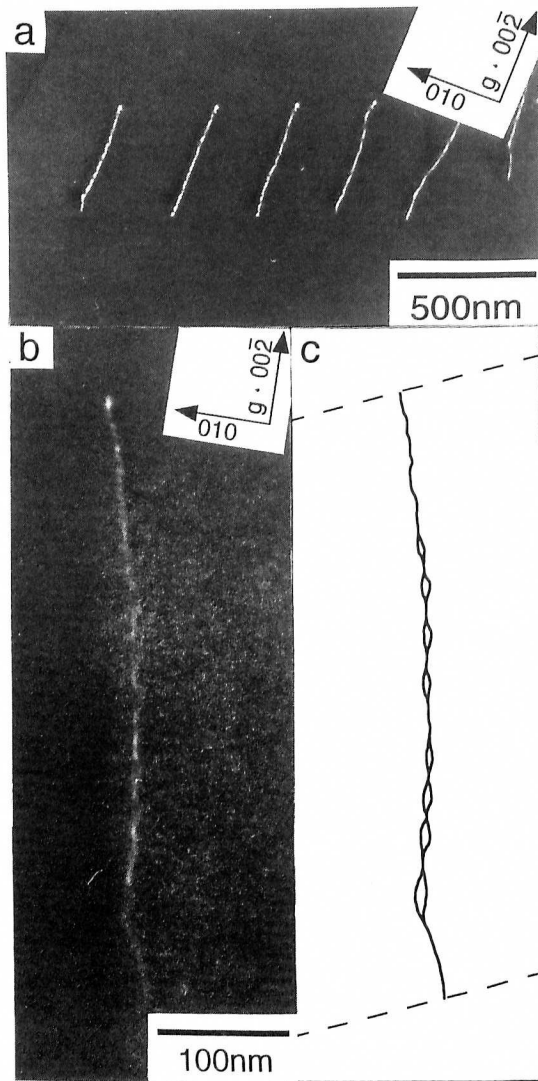


Fig.5 Dark field electron micrographs showing a dislocation array in  $(Al,Ni)_3Ti$  deformed at 773K. (b) magnified view of the dislocation, (c) schematic drawing of the dislocation.

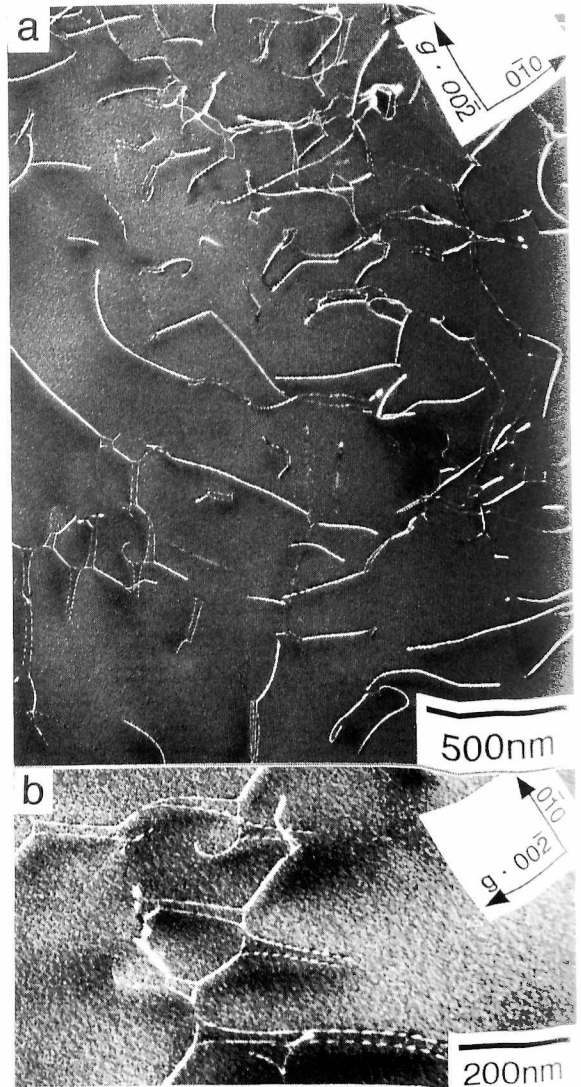
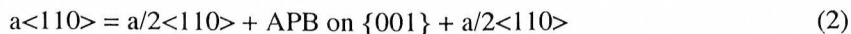


Fig.6 Dark field electron micrographs showing dislocations in  $(Al,Ni)_3Ti$  deformed at 1073K. (b) magnified view of dislocation nodes.

A dislocation array on a  $\{111\}$  plane is observed in the other grain of the same specimen (Fig. 5a). The dislocations in the array are screw dislocations of Burgers vector  $\mathbf{b}$ , which is parallel to  $\langle 110 \rangle$  on the  $\{111\}$  plane. Fig. 5b is a magnified view of a superdislocation in the array, appearing as a zigzag line. A schematic drawing is given in Fig. 5c. From a geometrical analysis by using the micrographs with different projection directions, it was found that the superdislocation is dissociated locally on a  $\{001\}$  plane. The local dissociation or cross slip on a  $\{001\}$  plane could produce significant obstacles for dislocations gliding on the  $\{111\}$  plane. For  $L1_2$ -trialuminides, no reports have ever been made of the direct observation of cross slip from a  $\{111\}$  onto a  $\{001\}$ . It is possible that the cross slip is the main reason for the measured positive temperature dependence of strength in the intermediate temperature range (Fig. 1) in the present  $L1_2$ - $(Al, Ni)_3Ti$ , in analogy with the K-W locking in  $L1_2$ - $Ni_3Al$ . Further investigation is needed to support the mechanism.

Figure 6 is dark field images showing dislocations in the specimens deformed to  $\sim 1\%$  at 1073K. Dislocation triple nodes are observed. They consist of undissociated dislocations and dissociated dislocations. The undissociated dislocations have a Burgers vector of  $\langle 100 \rangle$  type and the dissociated dislocations have a Burgers vector of  $\langle 110 \rangle$  type. A magnified view of nodes is shown in Fig. 6b. It was shown that a triple node is formed by the reaction of an undissociated  $a\langle 100 \rangle$  dislocation and a dissociated  $a\langle 110 \rangle$  dislocation according to the following equation.



The width of separation between the two  $a/2\langle 110 \rangle$  superpartials on  $\{001\}$  in Fig. 6b is measured to be  $20 \sim 30\text{nm}$ . This is much larger than the width of separation on  $\{111\}$ , which is often less than the width of dislocation images, typically a several nanometers. This result is consistent with the idea that APB energy in  $L1_2$  ordered structure is at minimum on  $\{001\}$ .

In the present  $L1_2$ - $(Al, Ni)_3Ti$  alloy, dislocations of  $a\langle 100 \rangle$  type, besides those of  $a\langle 110 \rangle$  type, are observed at all test temperatures employed. Turner et al. [5] observed dislocations of  $\langle 100 \rangle$  type in  $L1_2$ - $(Al, Ni)_3Ti$  alloy deformed at room temperature. While, for other  $L1_2$ - $(Al, X)_3Ti$  alloys,  $a\langle 100 \rangle$  dislocations has not been observed. Dislocations of  $a\langle 100 \rangle$  type, therefore, seem to be characteristic of the present alloy, but their roles in the deformation mechanisms are not known.

#### 4. SUMMARY

From the experimental results of compression test and transmission electron microscopic analysis, and discussion above, the results are summarized.

- (1) Yield strength of the  $(Al, Ni)_3Ti$  alloys decreases with increasing temperature in the low temperature range and increases slightly in the high temperature range.
- (2) A jerky flow is observed in compressive deformation at intermediate temperature ( $\sim 500\text{K}$ ) and with strain rate  $\sim 10^{-4}/\text{s}$ . The critical strain for the on set of jerky flow depends on strain rate and test temperature. The activation energy is estimated to be  $130\text{kJ/mol}$ .
- (3) Plastic deformation of these alloys occurs by the motion of superdislocations with  $a\langle 110 \rangle$  gliding on  $\{111\}$  planes.
- (4) Dissociation of superdislocations in  $(Al, Ni)_3Ti$  is of APB type on  $\{001\}$  plane at high temperature

(1073K).

#### **ACKNOWLEDGMENTS**

The present work was supported by The Light Metals Educational Foundation Inc., Osaka, Japan.

#### **REFERENCES**

- [1] K. Fukunaga, M. Kolbe, K. Yamada and Y. Miura: *Mat. Sci. Engin.*, A234-236(1997),594.
- [2] A. H. Cottrell : *Philo. Mag.*, ser. 7., 44(1953),829.
- [3] R. K. Ham and D. Jaffrey : *Philo. Mag.*, 15(1967),247.
- [4] M. Koiwa, H. Nakajima and T. Ito: *Bulletin of the Japan insitute of Met.*,28(1989),723.
- [5] C. D. Turner, W. O. Powers and J. A. Wert: *Acta metall.*, 37(1989),2635.